Applied Catalysis B: Environmental 158–159 (2014) 11–19

Contents lists available at ScienceDirect

Applied Catalysis B: Environmental

journal homepage: www.elsevier.com/locate/apcatb

Novel V_2O_5–CeO_2/TiO_2 catalyst with low vanadium loading for the selective catalytic reduction of NO_x by NH_3

Zhiming Liu[a,*], Shaoxuan Zhang[a], Junhua Li[b], Junzhi Zhu[a], Lingling Ma[c]

[a] State Key Laboratory of Chemical Resource Engineering, Beijing University of Chemical Technology, Beijing 100029, China
[b] School of Environment, Tsinghua University, Beijing 100084, China
[c] Key laboratory of Nuclear Analytical Techniques, Institute of High Energy Physics, Chinese Academy of Sciences, Beijing 100049, China

ARTICLE INFO

Article history:
Received 9 December 2013
Received in revised form 22 March 2014
Accepted 25 March 2014
Available online 2 April 2014

Keywords:
Nitrogen oxides
Selective catalytic reduction
VCeTi
Redox cycle

ABSTRACT

The effect of Ce on the activity and alkali resistance of V_2O_5/TiO_2 catalyst for the selective catalytic reduction (SCR) of NO_x by NH_3 has been investigated. It was found that the addition of Ce not only reduced the vanadium loading of V_2O_5/TiO_2 but also enhanced its activity and alkali resistance. The NO_x conversion over 0.5%V_2O_5-5%CeO_2/TiO_2 was much higher than that over 1%V_2O_5/TiO_2 catalyst. Based on the catalyst characterization, the redox cycle ($V^{4+} + Ce^{4+} \leftrightarrow V^{5+} + Ce^{3+}$) can account for the excellent NH_3-SCR catalytic performance of 0.5%V_2O_5–5%CeO_2/TiO_2 catalyst. In situ diffuse reflectance infrared transform spectroscopy (DRIFTS) measurements revealed that the role of Ce on the V_2O_5–CeO_2/TiO_2 catalyst was to contribute to the formation of NO_2 and monodentate nitrate species, both of which were reactive intermediates for the NH_3-SCR of NO_x.

1. Introduction

NO_x($NO + NO_2$) emission from stationary and mobile sources has been regarded as a major environmental concern [1]. Selective catalytic reduction of NO_x with ammonia (NH_3-SCR) has been proved to be one of the most successful methods to remove NO_x in the flue gas from stationary sources [1,2]. The conventional V_2O_5–$WO_3(MoO_3)/TiO_2$ catalyst is efficient for the NO_x control in the temperature range of 300–400 °C when it is applied to the flue gas from fossil fuels like oil and coal. With increasing attention to global warming, the use of biomass alone or as co-fuel has attracted attention because this type of fuel is considered CO_2 neutral. Unfortunately, the flue gas becomes very poisonous to the V_2O_5–$WO_3(MoO_3)/TiO_2$ catalyst due to the presence of alkaline potassium salts originating from the biomass combustion [3]. Fehrmann et al. [4] found that the K loading of 100 μmol/g led to a noticeable decrease of the activity of V_2O_5–$WO_3(MoO_3)/TiO_2$ catalyst. The deactivation was suggested to be due to the decreased reducibility of vanadia species [5]. Besides the poisoning effect of alkali metal, the toxicity of vanadium species is also one of the shortcomings. Therefore, developing novel NH_3-SCR catalyst with reduced vanadium and high activity and alkali resistance is desirable.

Recently, cerium based oxides have attracted much attention for their use as NH_3-SCR catalysts due to the high oxygen storage capacity and excellent redox property. Yang et al. [6,7] reported that MnO_x–CeO_2 mixed oxide was a superior catalyst for the low-temperature NH_3-SCR reaction. CrO_x–CeO_2 binary oxide also exhibited excellent NH_3-SCR activity [8]. The addition of Ce to V_2O_5–WO_3/TiO_2 led to the improved activity and alkali-resistance [9,10]. Chen et al. [9] attributed the activity enhancement to the synergetic interaction among V, W and Ce. For the Ce added V_2O_5–WO_3/TiO_2 catalyst, the loadings of W and Ce are relatively high [9,10]. Previous research showed that the synergetic effect between W and Ce can result in the high SCR performance [11,12]. Therefore, the synergetic effect between V and Ce needs to be clarified. Recently, the price of tungsten has risen about 30 times compared to ten years ago. SCR catalyst producer began to develop the substitute of tungsten [13]. Considering that the redox property is closely related to the NH_3-SCR performance [14], the combination of only V_2O_5 and CeO_2 is expected to show good SCR performance due to co-presence of the redox couples V^{5+}/V^{4+} and Ce^{4+}/Ce^{3+}. The absence of W would not only reduce the cost of the catalyst, but also lead to more strong interaction between V and Ce.

The present work attempts to improve the activity and alkali resistance of V_2O_5/TiO_2 catalyst with low vanadium loading by adding cerium oxide. Since H_2O is one of the main components in the flue gas from biomass combustion, the SCR activities of V1Ti and V0.5Ce5Ti catalysts in the presence of H_2O were also investigated. It was found that the addition of Ce exhibited a noticeable

* Corresponding author. Tel.: +86 10 64427356.
E-mail address: liuzm@mail.buct.edu.cn (Z. Liu).

http://dx.doi.org/10.1016/j.apcatb.2014.03.049
0926-3373/

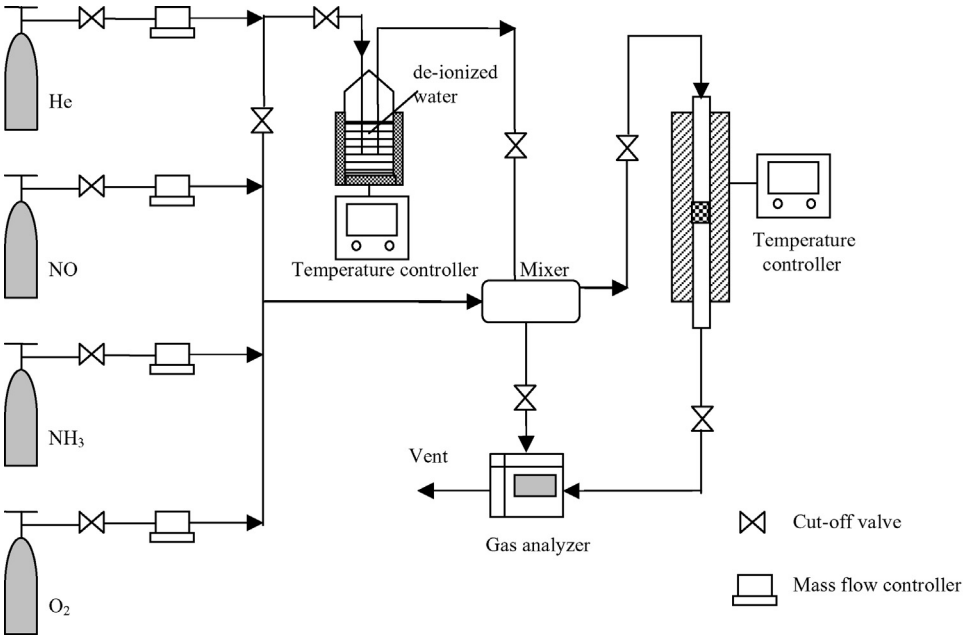

Fig. 1. Schematic diagram of the experimental setup.

promoting effect on the activity and alkali resistance of V_2O_5/TiO_2 for the NH_3-SCR. And V_2O_5–CeO_2/TiO_2 showed higher alkali-resistance than V_2O_5–WO_3/TiO_2 catalyst. On the basis of the characterization results, the cause of the promoting effect of Ce has been elucidated.

2. Experimental

2.1. Catalyst preparation

The catalysts were prepared by the impregnation method, and Degussa AEROSIL TiO_2 P25 was used as the support. VxTi (VxTi = x% V_2O_5/TiO_2, x is the ratio of $V_2O_5/V_2O_5 + TiO_2$) catalyst was prepared by impregnating TiO_2 with a proper amount of ammonium metavanadate (NH_4VO_3) and oxalic acid solution, then stirred for 4 h, subsequently dried at 120 °C and calcined at 500 °C for 4 h in air. Ce5Ti (Ce5Ti = 5%CeO_2/TiO_2, weight percentage of CeO_2 is the ratio of $CeO_2/CeO_2 + TiO_2$) was prepared by the same method as described above using cerium nitrate ($Ce(NO_3)_3{\cdot}6H_2O$) solution instead. VxCe5Ti (VxCe5Ti = x%V_2O_5–5%CeO_2/TiO_2) catalyst was prepared by impregnating Ce5Ti powder with an oxalic acid solution of NH_4VO_3. After stirring for 4 h, the suspension was dried at 120 °C and then calcined at 500 °C for 4 h in air. The state-of-the art SCR V0.5W5Ti (V0.5W5Ti = 0.5%V_2O_5–5%WO_3/TiO_2) catalyst was also prepared by the same preparation method as described above using NH_4VO_3 and $(NH_4)_{10}W_{12}O_{41}$ as precursors ($H_2C_2O_4{\cdot}2H_2O$ was used to facilitate the solution of the precursors) and TiO_2 as the support.

The potassium doped VxCe5Ti, VxTi and V0.5W5Ti catalysts with different potassium loading were prepared by impregnating these catalysts of 40–60 mesh with the aqueous solutions containing the required amount of KNO_3, then dried in air and calcined at 500 °C for 4 h. The K loading was calculated by the weight of K to that of VxCe5Ti, VxTi and V0.5W5Ti, respectively.

2.2. Catalytic activity measurement

The activity measurements were carried out in a fixed-bed quartz reactor using a 0.12 g catalyst of 40–60 mesh. The schematic diagram of the experimental setup was shown in Fig. 1. The feed gas mixture contained 500 ppm NO, 500 ppm NH_3, 5% O_2, 0 or 5% H_2O and helium as the balance gas. Water vapor was generated by passing helium gas through a heated gas-wash bottle containing de-ionized water. The required percentage of water can be controlled by changing the temperature of the de-ionized water, which was monitored by a temperature controller. The total flow rate of the feed gas was 300 $cm^3\ min^{-1}$, corresponding to a GHSV of 128,000 h^{-1}. The reaction temperature was increased from 200 to 450 °C in a heating rate of 5 °C min^{-1}. The composition of the gas in the inlet and outlet streams was analyzed by a chemiluminescence NO/NO_2 analyzer (Thermal Scientific, model 42i-HL) and gas chromatograph (Shimadzu GC 2014 equipped with Porapak Q and Molecular sieve 5A columns). A molecular-sieve 5A column was used for the analysis of N_2 and Porapak Q column for that of N_2O. The activity data were collected when the catalytic reaction practically reached steady-state condition at each temperature. No N_2O was detected and all the NO_x were converted into N_2 for the investigated catalysts. All the experiment in this work, the nitrogen balance is more than 95%.

2.3. Catalyst characterization

Characterization of the BET surface area of the samples was carried out with a Quantachrome Autosorb AS-1 system. Prior to the surface area measurement, the sample was degassed in vacuum at 400 °C for 4 h. The elemental analysis of the samples was performed by inductively coupled plasma atomic emission spectroscopy (ICP) on a Plasma-Spec-I spectrometer.

Powder X-ray diffraction (XRD) measurements were recorded on a Brucker D8 ADVANCE system with Cu $K\alpha$ radiation at 45 kV and 200 mA. XPS measurements were conducted on an ESCALab220i-XL electron spectrometer from VG Scientific using 300 W Mg $K\alpha$ radiation, calibrated internally by carbon deposit C 1s binding energy (BE) of 284.8 eV. A least-square routine of peak fitting was used for the analysis of XPS spectra. Temperature programmed reduction of H_2 (H_2-TPR) and temperature programmed desorption of NH_3 (NH_3-TPD) were performed on a chemisorption analyzer (Micromeritics, ChemiSorb 2720 TPx). For H_2-TPR, the sample was under a 10% H_2 gas flow (50 $cm^3\ min^{-1}$) at a rate of 10 °C min^{-1} up to 800 °C. For NH_3-TPD, the sample was pretreated at 300 °C in He

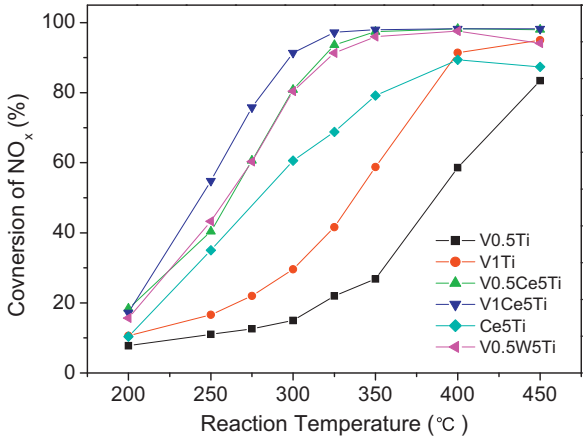

Fig. 2. NO_x conversion as a function of reaction temperature over various catalysts. Reaction conditions: [NO] = [NH_3] = 500 ppm, [O_2] = 5%, GHSV = 128,000 h^{-1}.

for 1 h, then it was cooled down and exposed in a 500 ppm NH_3/He gas flow for 1 h, followed by flushing with He for 30 min, the sample was then heated up to 550 °C with a rate of 10 °C min^{-1} in flowing He.

In-situ DRIFTS spectra were recorded using a thermo Nicolet 6700 spectrometer equipped with a high temperature environmental cell fitted with ZnSe window and a MCT detector cooled with liquid N_2. The catalyst was loaded in the Harrick IR cell and heated to 400 °C under helium at a total flow rate of 100 cm^3 min^{-1} for 60 min to remove adsorbed impurities. A background spectrum was collected under a flowing helium atmosphere and was subtracted from the sample spectra. The DRIFTS spectra were recorded by accumulating 100 scans with a resolution of 4 cm^{-1}.

3. Results and discussion

3.1. NH_3-SCR activity

NH_3-SCR activities of VxTi, Ce5Ti, VxCe5Ti and V0.5W5Ti catalysts as a function of temperature were evaluated and the results are illustrated in Fig. 2. It can be seen that the V1Ti catalyst exhibited higher NH_3-SCR activity than V0.5Ti catalyst. This is in accordance with the previous report by Fehrmann et al. [15] that the relatively high vanadium loading contributed to improving the SCR activity. The addition of 5%CeO_2 significantly enhanced the NO_x conversion of both V0.5Ti and V1Ti catalysts. Only 15 and 30% NO_x conversion were obtained at 300 °C over V0.5Ti and V1Ti catalysts, respectively. In contrast, the NO_x conversion was improved to 81 and 91% after doping 5% CeO_2 on these two catalysts. At 250 °C, the NO_x conversion over V0.5Ce5Ti catalyst is 40%, which is lower than that of V0.1W6Ce10Ti catalyst reported by Chen et al. [9]. The much higher space velocity (128,000 vs 28,000 h^{-1}) and the absence of W could be the reasons for the lower NO_x conversion in this study. Both the T_{50} and T_{90} of V0.5Ce5Ti catalyst were significantly lower than those of V1Ti and Ce5Ti catalysts (see Table 1). Therefore, V0.5Ce5Ti was much more active than V1Ti and Ce5Ti catalysts. This fact indicated that the co-existence of V and Ce contributed to improving the SCR activity. V0.5Ce5Ti exhibited similar activity to that of V0.5W5Ti catalyst, indicating that Ce could be the substitute of W for the promoter of VTi catalyst. Considering that V0.5Ce5Ti with lower vanadium loading was active, we focused on this catalyst in the comparison with V1Ti catalyst.

Table 1
Comparison of the reaction temperature over different catalysts.

Catalyst	Temperature (°C)[a]		
	T_{10}	T_{50}	T_{90}
V0.5Ti	233	386	–
V1Ti	200	338	396
V0.5Ce5Ti	–	262	320
V1Ce5Ti	–	233	298
Ce5Ti	200	280	400

[a] T_{10}, T_{50} and T_{90} represents the temperature at which the conversion of NO_x was 10%, 50% and 90%, respectively.

Table 2
The loading of K detected by ICP over different catalysts.

Catalyst	K (wt.%)
V1Ti/0.1 K	0.09
V1Ti/0.2 K	0.18
V0.5Ce5Ti/0.1 K	0.09
V0.5Ce5Ti/0.2 K	0.19
V0.5W5Ti/0.2 K	0.19

3.2. Effect of H_2O

As shown in Fig. S1, NO_x conversion over V1Ti catalyst was seldom changed due to the presence of H_2O. Although the presence of H_2O led to the decrease of the NO_x conversion over V0.5Ce5Ti catalyst in the temperature range of 200–400 °C, the conversion was much higher than that obtained over V1Ti catalyst. This fact indicated that V0.5Ce5Ti catalyst was still more active for the NO_x reduction by NH_3 in the presence of H_2O, which is very important for the practical application.

3.3. Effect of alkali metal

The actual amount of the doped K on the catalysts is listed in Table 2. It can be seen that the loading of K analyzed by ICP is slightly lower than the theoretical value. Fig. 3 showed the conversion of NO_x as a function of reaction temperature over potassium doped V0.5Ce5Ti and V1Ti catalysts. It is evident that the doped K led to a noticeable decrease of NO_x conversion in the whole temperature region investigated. For V1Ti catalyst, the NO_x conversion at 350 °C was decreased to 37% after doping 0.1% K, and the conversion was further decreased with potassium loading increased to 0.2%. The doped potassium also led to the decreased activity of V0.5Ce5Ti catalyst. However, much higher NO_x conversion than

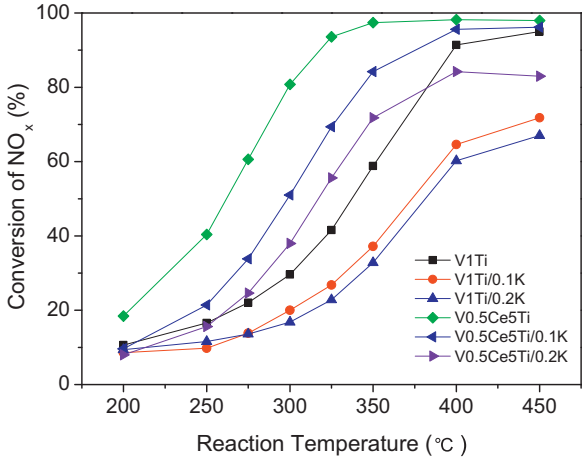

Fig. 3. The effect of potassium on NO_x conversion over V0.5Ce5Ti and V1Ti catalysts. Reaction conditions: [NO] = [NH_3] = 500 ppm, [O_2] = 5%, GHSV = 128,000 h^{-1}.

Table 3
Effect of K on the reaction temperature of different catalysts.

Catalyst	Temperature (°C)[a]		
	T_{10}	T_{50}	T_{90}
V1Ti	200	338	396
V1Ti/0.1 K	247	372	–
V1Ti/0.2 K	248	381	–
V0.5Ce5Ti	–	262	320
V0.5Ce5Ti/0.1 K	212	298	375
V0.5Ce5Ti/0.2 K	220	320	–

[a] T_{10}, T_{50} and T_{90} represents the temperature at which the conversion of NO_x was 10%, 50% and 90%, respectively.

Table 4
Ratio of the decreased activity due to the doped K over the different catalysts[a].

Catalyst	Ratio of the decreased activity (%)				
	300 °C	325 °C	350 °C	400 °C	450 °C
V1Ti/0.1 K	32.4	35.6	36.7	26.8	24.4
V0.5Ce5Ti/0.1 K	36.8	25.8	13.6	2.6	1.8
V1Ti/0.2 K	43.2	45.2	44.2	34.1	29.5
V0.5Ce5Ti/0.2 K	52.0	40.5	26.2	14.3	15.3

[a] Ratio of the decreased activity = [(NO_x conversion over the fresh catalyst) − (NO_x conversion over the poisoned catalyst)]/NO_x conversion over the fresh catalyst.

V1Ti was obtained in the whole temperature range. NO_x conversion of 84% was achieved at 350 °C over V0.5Ce5Ti catalyst doped with 0.1% potassium. Below 400 °C, V0.5Ce5Ti catalyst doped with 0.2% potassium was even more active than the fresh V1Ti catalyst. Compared with the K doped V1Ti catalyst, both the T_{10} and T_{50} of K doped V0.5Ce5Ti were decreased significantly (see Table 3). Table 4 listed the ratios of the decreased activity due to the doped K over V1Ti and V0.5Ce5Ti catalysts. Except for at 300 °C, the ratios of the decreased activity for V0.5Ce5Ti are lower than those for V1Ti catalyst, which is more pronounced at higher temperatures. This fact suggested that the presence of Ce contributed to improving the alkali-resistance of VTi catalyst above 300 °C.

To better evaluate the alkali resistance of V0.5Ce5Ti catalyst, we also carried out the comparative SCR activity test over K doped V0.5Ce5Ti and V0.5W5Ti catalysts (see Fig. 4). Compared with K doped V0.5W5Ti, K doped V0.5Ce5Ti exhibited much higher NO_x conversion in the whole temperature range investigated. Therefore, VCeTi is more applicable than VWTi catalyst for the control of NO_x in the biomass fired flue gas.

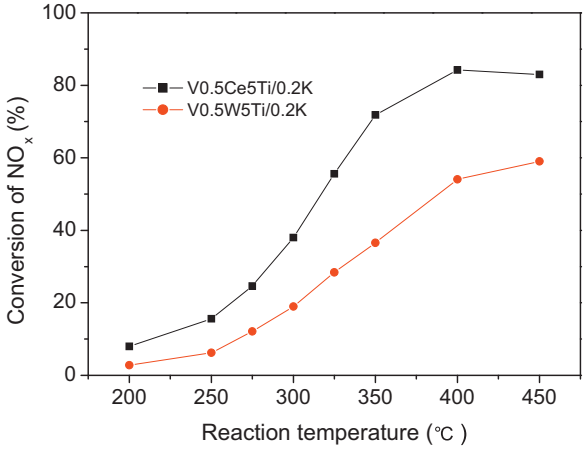

Fig. 4. Comparison of the NH_3-SCR activity of K doped V0.5Ce5Ti and V0.5W5Ti catalysts. Reaction conditions: [NO] = [NH_3] = 500 ppm, [O_2] = 5%, GHSV = 128,000 h^{-1}.

Table 5
BET surface area of different catalysts.

Catalyst	BET surface area (m^2/g)
V1Ti	46.5
Ce5Ti	52.9
V0.5Ce5Ti	44.6

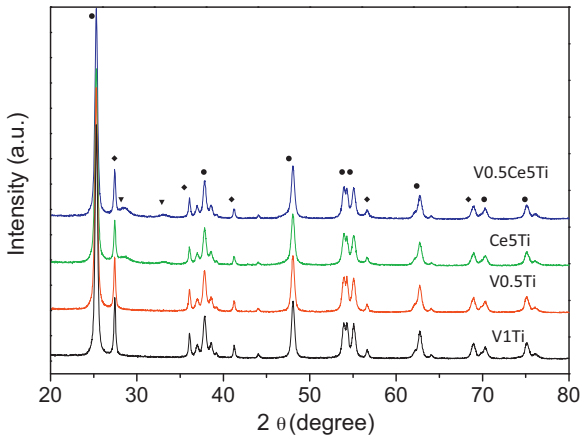

Fig. 5. XRD patterns of various catalysts. (●) Anatase TiO_2; (♦) Rutile TiO_2; (▼) Cubic CeO_2.

3.4. BET surface area and XRD patterns

As shown in Table 5, the BET surface area followed in the order of Ce5Ti > V1Ti > V0.5Ce5Ti. Although the BET surface area of V0.5Ce5Ti was the lowest, it exhibited the highest NH_3-SCR activity, indicating that some synergistic effect existed between Ce and V species and the BET surface area did not play a key role in the SCR reaction.

Fig. 5 showed the XRD patterns of different catalysts. For all the catalysts, the anatase phase was the main phase [12], and only a little rutile phase (PDF-ICDD21-1276) was detected. The peak assigned to V_2O_5 was absent, suggesting that V_2O_5 was highly dispersed on the surface of TiO_2. For Ce5Ti and V0.5Ce5Ti catalysts, a weak peak ascribed to CeO_2 was observed [16].

3.5. NH_3-TPD

Fig. 6 illustrated the NH_3-TPD profiles of the fresh and poisoned V1Ti and V0.5Ce5Ti catalysts. Both the fresh V1Ti and V0.5Ce5Ti

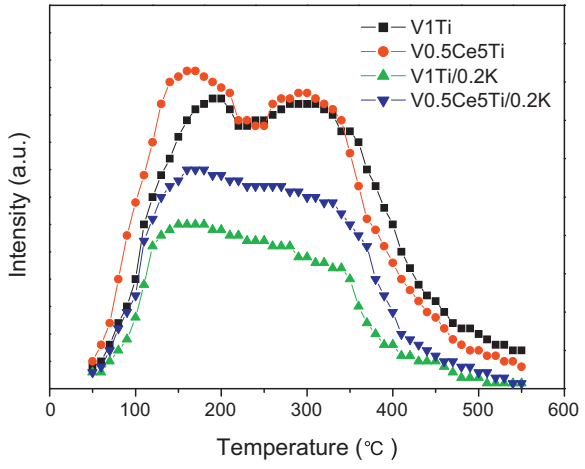

Fig. 6. NH_3-TPD profiles of the fresh and poisoned V1Ti and V0.5Ce5Ti catalysts.

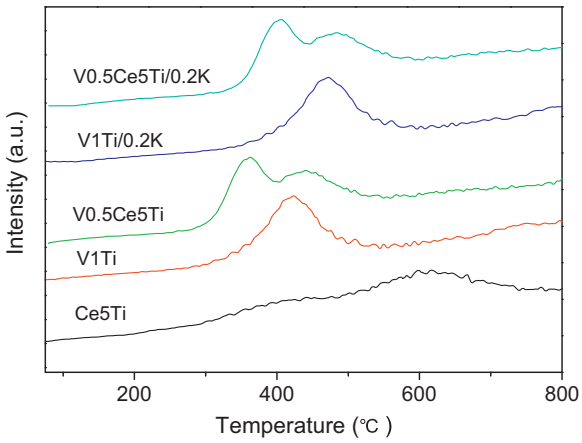

Fig. 7. H_2-TPR profiles of Ce5Ti, V1Ti, V0.5Ce5Ti, K-doped V1Ti and V0.5Ce5Ti catalysts.

catalysts exhibited two NH_3 desorption peaks around 180 and 300 °C, which can be attributed to the weakly bonded and strongly bonded NH_3, respectively [17]. Compared to the fresh catalyst, the NH_3 desorption decreased after doping K. The amount of NH_3 desorbed calculated from the desorption peak are 183, 189, 88 and 126 μmol g^{-1} for V1Ti, V0.5Ce5Ti, K-doped V1Ti and K-doped V0.5Ce5Ti catalysts, respectively. The doping K led to the decrease of the NH_3 adsorption, and thus lowered the SCR performance. More desorbed NH_3 over K-doped V0.5Ce5Ti than K-doped V1Ti catalyst could be one reason for its higher SCR performance.

3.6. Redox properties

Temperature-programmed reduction (H_2-TPR) analysis was conducted to investigate the reduction behavior of V1Ti, V0.5Ce5Ti and Ce5Ti catalysts. As illustrated in Fig. 7, V1Ti catalyst showed a hydrogen consumption peak at 423 °C, which is attributed to the reduction of V^{5+} [18]. Ce5Ti exhibited two reduction peaks at around 420 and 600 °C. The former peak is probably assigned to the reduction of the surface oxygen of ceria and the second one is due to the reduction of Ce^{4+} to Ce^{3+} [19,20]. V0.5Ce5Ti exhibited two peaks at 360 and 440 °C, which could be assigned to the reduction of V^{5+} and Ce^{4+}, respectively. It is evident that the reduction temperatures of V^{5+} and Ce^{4+} were both decreased, indicating that the vanadium and ceria oxides became more reducible, which can be ascribed to the synergetic effect between V and Ce. While for VWTi catalyst, the reducibility change of V due to the addition of Ce was not evident [9]. This fact indicates that in the absence of W the interaction between V and Ce becomes stronger. For the K-doped V1Ti catalyst, the reduction peak of V species shifted to higher temperatures by about 50 °C. The reduction peaks of V^{5+} and Ce^{4+} were also moved to higher regions by about 40 °C for the K-doped V0.5Ce5Ti catalyst. These results suggest that the doped K decreased the reducibility of the catalyst, thus leading to the deactivation.

In order to elucidate the surface nature of the active sites over the catalyst systems X-ray photoelectron spectra (XPS) analysis was conducted. The complex spectrum of Ce3d was decomposed into eight components with the assignment defined in Fig. 8(a). The sub-bands labeled u′ and v′ represent the $3d^{10}4f^1$ initial electronic state corresponding to Ce^{3+}, and those labeled u, u″, u‴, v, v″ and v‴ represent the $3d^{10}4f^0$ initial electronic state corresponding to Ce^{4+} [12]. The ratio of Ce^{3+} on V0.5Ce5Ti catalyst is 31.62%. In the case of V0.1W6Ce5Ti catalyst, Ce was found to be present mainly in the form of Ce^{3+} [9]. Therefore, the absence of W could contribute to the formation of redox couple of Ce^{4+}/Ce^{3+}.

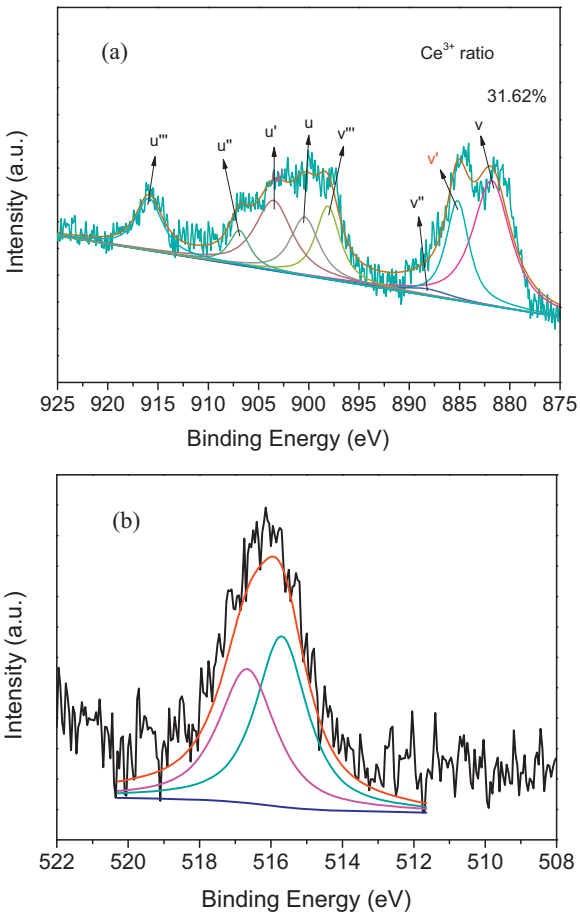

Fig. 8. Ce3d(a) and V2p(b) XPS spectra of V0.5Ce5Ti catalyst.

By performing a peak fitting deconvolution, the V2p spectra can be separated into two characteristic peaks centered at 515.6 and 517.1 eV, which were ascribed to V^{4+} and V^{5+}, respectively (see Fig. 8(b)) [21,22]. The redox couple V^{5+}/V^{4+} could transfer electrons to Ce^{4+}, thus leading to Ce^{4+} more reducible as shown in the H_2-TPR profile.

As shown in Fig. 9, the O1s peak was fitted into two sub-bands: the peak at 529.7 eV corresponds to the lattice oxygen O^{2-} (denoted as O_β) and the one at 531.2 eV corresponds to the surface adsorbed oxygen (denoted as O_α) such as O_2^{2-} or O^- belonging to defect oxide or hydroxyl-like species [23,24]. It is evident that the ratio

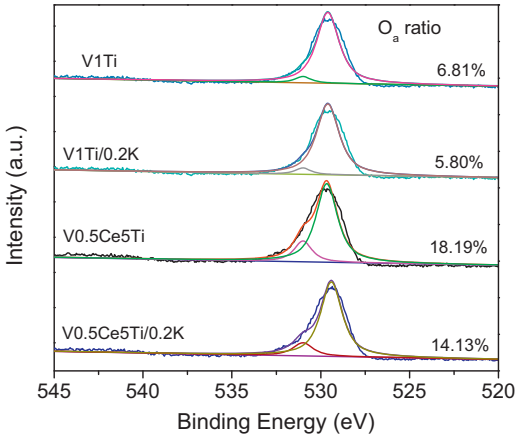

Fig. 9. XPS spectra of O1s for different catalysts.

Table 6
Assignments of DRIFTS bands observed during the adsorption of NH_3.

Wavenumber (cm^{-1})	Assignments	References
3350, 3248 and 3155	N—H stretching vibration modes of the coordinated NH_3	[28]
1594, 1250 and 1172	Asymmetric and symmetric bending vibrations of the coordinated NH_3 linked to Lewis acid sites	[26,27]
1450	Asymmetric and symmetric bending vibrations of NH_4^+ species on Brønsted acid sites	[29]

of O_α over V0.5Ce5Ti was much higher than that over V1Ti catalyst (18.19% vs 6.81%). The existence of Ce^{3+} could create charge imbalance, the vacancies and unsaturated chemical bonds on the catalyst surface, leading to more surface chemisorbed oxygen formed over V0.5Ce5Ti catalyst. The surface chemisorbed oxygen O_α was reported to be highly active for the NH_3-SCR [23,25]. The doping of K led to the decrease of the ratio of O_α over both V1Ti and V0.5Ce5Ti catalysts, but the ratio of O_α over K-doped V0.5Ce5Ti was noticeably higher than that of V1Ti catalyst. The lower concentration of surface chemisorbed oxygen could cause the less reactive oxidation process, thus decreasing the SCR activity. The ratio of O_α over the fresh V1Ti catalyst is lower than that of K-doped V0.5Ce5Ti catalyst, but its activity is higher than that of K-doped V0.5Ce5Ti catalyst above 400 °C (see Fig. 2). This fact indicates that the surface chemisorbed oxygen may be important for the SCR performance at relatively low temperatures. At high temperatures the oxidative process is more easily to proceed and the role of the surface oxygen becomes unimportant. And besides the surface oxygen, some other property, such as the surface acidity, could play an important role for the SCR performance.

3.7. *In situ DRIFTS studies*

It is expected that the addition of CeO_2 will affect the formation of reactive intermediates, and hence the NH_3-SCR activity of V_2O_5/TiO_2 catalyst. Therefore, in situ diffuse reflectance infrared transform spectroscopy (DRIFT) experiments were conducted to elucidate the mechanistic cause of the promoting effect of CeO_2.

3.7.1. *Adsorption of NH_3*

Fig. 10(a) showed the DRIFT spectra of NH_3 adsorption over V1Ti catalyst at different temperatures. The bands at 1594 and 1250, 1172 cm^{-1} can be assigned to asymmetric and symmetric bending vibrations of the coordinated NH_3 linked to Lewis acid sites [26,27], and that at 3350, 3248 and 3155 cm^{-1} can be ascribed to the N-H stretching vibration modes of the coordinated NH_3 [28]. The band at 1450 cm^{-1} could be attributed to asymmetric and symmetric bending vibrations of NH_4^+ species on Brønsted acid sites [29]. With increasing temperature, the intensity of the bands assigned to NH_4^+ species on Brønsted acid sites decreased faster than that of the bands due to NH_3 linked to Lewis acid sites. This indicates that ammonia bonded to Lewis acid sites were more stable than that on Brønsted acid sites [30]. The DRIFT spectra of NH_3 adsorption over V0.5Ce5Ti catalyst are shown in Fig. 10(b). From the comparison of Fig. 10(a) and (b), it can be seen that the DRIFT spectra of NH_3 adsorption on V0.5Ce5Ti catalyst were similar to that of V1Ti catalyst. The assignments of DRIFTS bands were summarized in Table 6.

The DRIFT spectra of NH_3 adsorption over 0.2%K-doped V1Ti and V0.5Ce5Ti catalysts at different temperatures are illustrated in Fig. 11. Compared with Fig. 10, it is evident that the intensities

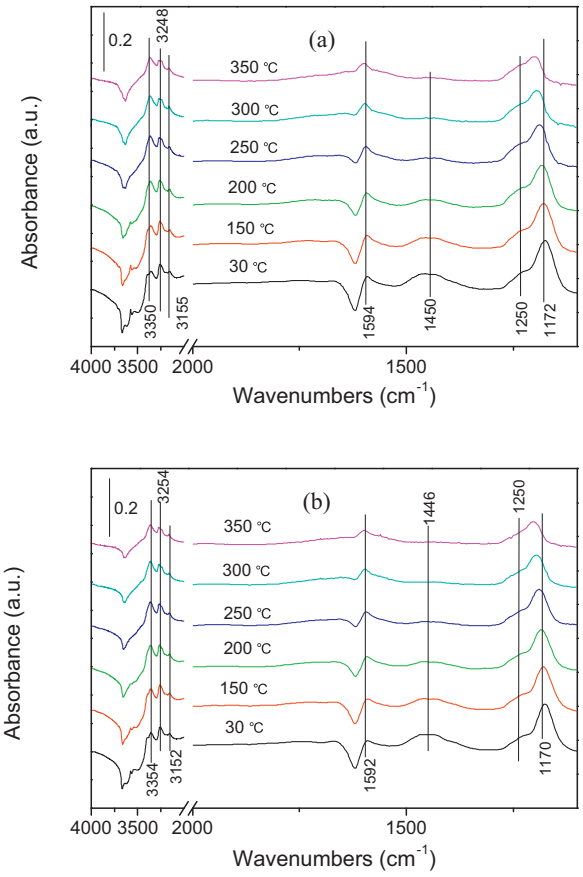

Fig. 10. DRIFT spectra of V1Ti(a) and V0.5Ce5Ti(b) treated in flowing 500 ppm NH_3 at room temperature for 60 min and then purged by He at 30, 150, 200, 250, 300, and 350 °C.

of the peaks ascribed to adsorbed ammonia on Lewis acid sites and Brönsted acid sites over V1Ti and V0.5Ce5Ti catalysts were both decreased due to the doped K. The decreased adsorption of NH_3 led to the lower SCR activity. Above 250 °C, the peak ascribed to coordinated NH_3 linked to Lewis acid sites over K-doped V0.5Ce5Ti was much higher than K-doped V1Ti catalyst (see Fig. 11). More adsorbed NH_3 contributed to the NH_3-SCR to proceed. Consequently, the NH_3 adsorption results were quite correlated with SCR activity trend as shown in Fig. 2.

3.7.2. *Co-adsorption of NO and O_2*

The DRIFT spectra of $NO + O_2$ over V1Ti catalyst at different temperatures were shown in Fig. 12(a). Several distinct bands appeared at 1609, 1580, 1488, 1292, and 1241 cm^{-1}, which were assigned to the asymmetric frequency of gaseous NO_2 molecules (1609 cm^{-1}) [30], bidentate nitrate (1580 cm^{-1}) [31], monodentate nitrate (1488 and 1292 cm^{-1}) [32] and bridged nitrate (1241 cm^{-1}) [33], respectively. With increasing temperature, the intensity of the band at 1292 cm^{-1} decreased and it vanished above 200 °C, while the band at 1488 cm^{-1} shifted to 1547 cm^{-1}, which was also ascribed to monodentate nitrate [34]. From 250 °C a new band at 1355 cm^{-1} appeared, which can be assigned to cis-$N_2O_2^{2-}$ [7]. Table 7 listed the assignments of the DRIFTS bands.

Compared with the co-adsorption of $NO + O_2$ on V1Ti catalyst, similar adsorption bands were observed on V0.5Ce5Ti catalyst (see Fig. 12(b)). However, the intensities of the bands assigned to nitrate species and gaseous NO_2 were noticeably increased over the latter catalyst, which indicated that the presence of Ce contributed to the formation of nitrate species and NO_2.

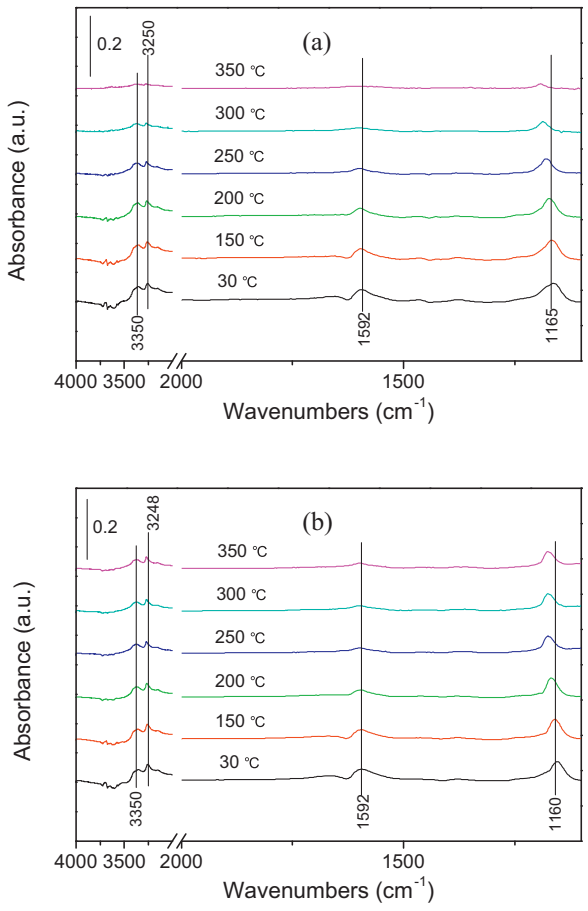

Fig. 11. DRIFT spectra of 0.2% K-doped V1Ti(a) and V0.5Ce5Ti(b) treated in flowing 500 ppm NH_3 at room temperature for 60 min and then purged by He at 30, 150, 200, 250, 300, and 350 °C.

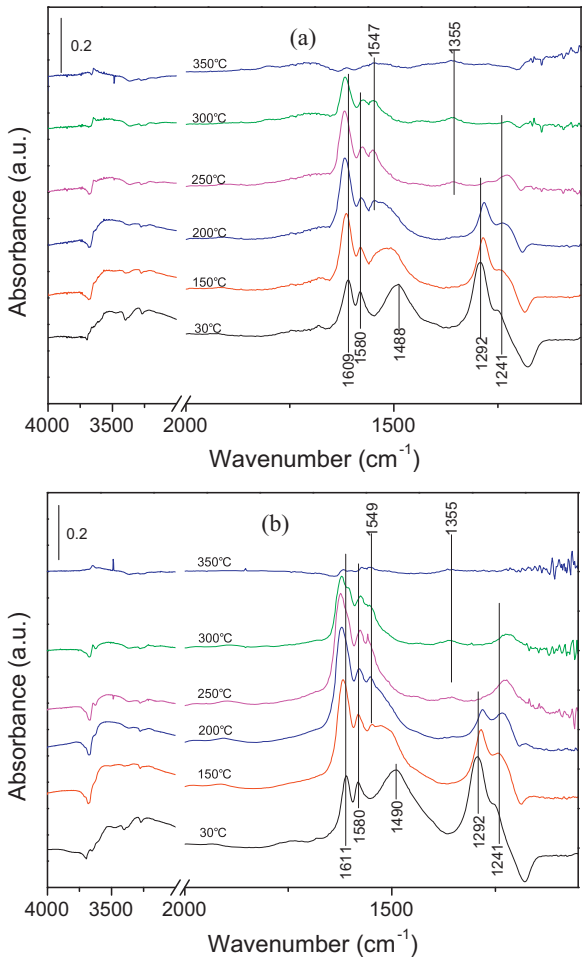

Fig. 12. DRIFT spectra of V1Ti(a) and V0.5Ce5Ti(b) treated in flowing 500 ppm NO + 5% O_2 at room temperature for 60 min and then purged by He at 30, 150, 200, 250, 300, and 350 °C.

Table 7
Assignments of DRIFTS bands observed during the co-adsorption of NO and O_2.

Wavenumber (cm^{-1})	Assignments	References
1609	Asymmetric frequency of gaseous NO_2 molecules	[30]
1580	Bidentate nitrate	[31]
1488, 1292 and 1547	Monodentate nitrate	[32,34]
1355	Cis-$N_2O_2^{2-}$	[7]
1241	Bridged nitrate	[33]

3.7.3. *Reaction between ammonia and adsorbed nitrogen oxides species*

Chen et al. [9] found that nitrates were formed due to the addition of Ce over VWTi catalyst [9]. However, the reactivities of the different nitrates have not been differentiated. The reactivity of the adsorbed nitrate and NO_2 species toward NH_3 over V1Ti and V0.5Ce5Ti was studied by the transient response of the DRIFT spectra. Fig. 13 showed the in situ DRIFT spectra of V1Ti and V0.5Ce5Ti catalysts in a flow of NH_3 after the catalysts was pre-exposed to a flow of NO + O_2 for the 60 min followed by helium purging for 30 min at 250 °C. Switching the gas to NH_3 in 2 min led to the disappearance of the bands at 1613 and 1545 cm^{-1} related to NO_2 and monodentate nitrate, respectively (see Fig. 13(a)) [30,34]. And meanwhile the coordinated NH_3 (1181 and 1600 cm^{-1}) and NH_4^+ (1437 cm^{-1}) formed. This fact indicated that both NO_2 and monodentate nitrate species were reactive intermediates in the NH_3-SCR process.

As illustrated in Fig. 13(b), the intensities of both bidentate nitrate and bridged nitrate seldom changed after exposing NH_3 flow even for 60 min, indicating that these two species were spectator species for the NH_3-SCR. The bands assigned to NO_2 and monodentate nitrate disappeared after exposing V0.5Ce5Ti catalyst to NH_3 flow for 2 min, which was similar to the case on V1Ti catalyst.

According to the mechanism proposed by Topsøe [14,35], the catalytic cycle consists of four steps: first, adsorption of NH_3 on the Brönsted acid sites (V—OH) to form —NH_4^+; second, oxidation of the —NH_4^+ by adjacent V^{5+}=O to form —NH_3^+ and reduction of V^{5+}=O to V^{4+}—OH; third, reaction of the —NH_3^+ with the gas phase NO to form —NH_3^+NO and decomposition of —NH_3^+NO into N_2 and H_2O; finally, V^{4+}—OH was re-oxidized to V^{5+}=O by O_2. The redox couples of V^{4+}/V^{5+} seemed to play an important role for the SCR reaction to proceed. Based on the XPS characterization, it can be seen that high ratio of Ce^{3+} exist over V0.5Ce5Ti catalyst. The existence of Ce^{3+} can contribute to the redox process of V^{4+}/V^{5+}. Therefore, the redox cycle ($V^{4+} + Ce^{4+} \leftrightarrow V^{5+} + Ce^{3+}$) exists over V0.5Ce5Ti catalyst and the electron transfer can be facilitated as follows:

$$Ce^{4+}—O^{2-}—V^{5+} + e \leftrightarrow Ce^{4+}—O^{2-}—V^{4+} \leftrightarrow Ce^{3+}—O^{2}—V^{5+}$$
$$\leftrightarrow Ce^{4+}—O^{2-}—V^{5+} + e$$

The redox cycle resulted in a decrease in the energy required for the electron transfer between Ce and V active sites, promoting the activation of NH_3 and NO, and consequently an improvement of the NH_3-SCR activity. Due to the existed redox cycle, the vanadia

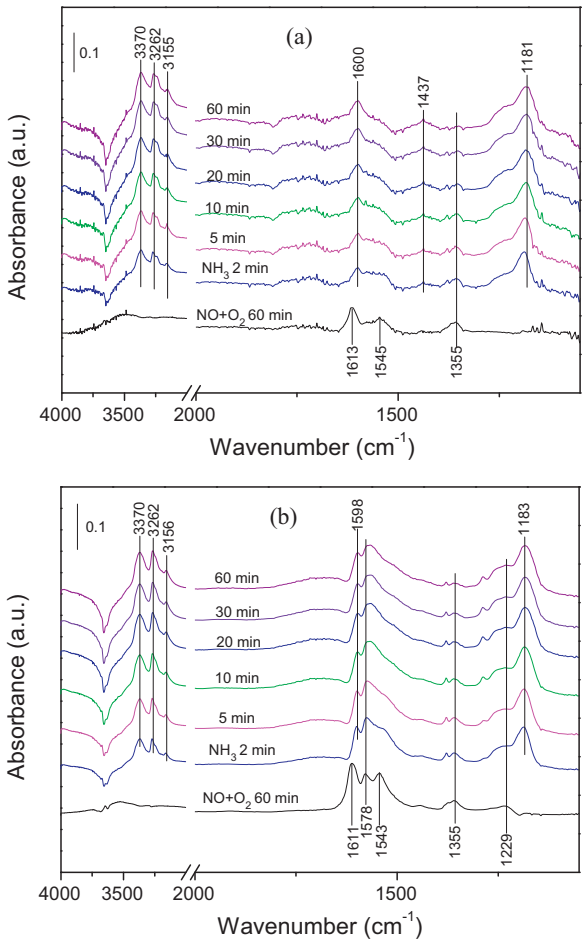

Fig. 13. Dynamic changes of the in situ DRIFT spectra over V1Ti(a) and V0.5Ce5Ti (b) catalysts as a function of time in a flow of NH_3 after the catalysts was pre-exposed to a flow of NO + O_2 for the 60 min followed by helium purging for 30 min at 250 °C.

species on the K-doped V0.5Ce5Ti is even more reducible than that of the fresh V1Ti catalyst. On the other hand, the presence of Ce^{3+} induced the formation of more surface oxygen species(O_α), which was beneficial for the NH_3-SCR reaction. After doping K, the ratio of O_α over V0.5Ce5Ti was still much higher than that of V1Ti catalyst. The adsorption of NH_3 was also less affected over V0.5Ce5Ti catalyst due to the doping of K. All these could be responsible for the high alkali resistance of V0.5Ce5Ti catalyst.

As to the mechanism of the NH_3-SCR reaction, different hypothesis have been proposed [36–39], including the reaction between an amide and gaseous NO, the reaction between ammonium ion and adsorbed NO_2, and the reaction between coordinated ammonia and a species generated by spillover on the support. However, the roles of the nitrate species in the SCR process need to be studied extensively. Chen et al. [30] found that nitrate species were not reactive to react with NH_3 over CeWTi catalyst. Kijlstra et al. [40] proposed that the thermally stable nitrate species can cover the surface active sites to prevent the reactants (NH_3 or/and NO) from further adsorption and reaction, and thus resulted in the deactivation of the catalyst. Besides nitrate species, NO_2 was considered to be an important intermediate species for the SCR reaction [7]. Koebel et al. [41] investigated the low temperature behavior of the NH_3-SCR process over V_2O_5/TiO_2 catalyst with feed gases containing both NO and NO_2. The mixture feeding improved the reaction rate significantly compared with feeding NO. In the present study, both adsorbed NO_2 and monodenate nitrate were reactive and they can react with adsorbed NH_3 following the Langmuir–Hinshelwood-type reaction [40], whereas bidentate nitrate and bridged nitrate were spectator species. The addition of Ce to VTi catalyst contributed to the formation of monodenate nitrate and NO_2. Moreover, the formation of NO_2 could also re-oxidize V^{4+} to V^{5+}, which was done by O_2 as reported by Ramis et al. [42], thus promoting the redox cycle. As a result, V0.5Ce5Ti catalyst exhibited higher catalytic performance for the NH_3-SCR than V1Ti catalyst.

4. Conclusions

Novel VCeTi catalyst with a lower vanadium loading for the selective catalytic reduction of NO_x has been developed. V0.5Ce5Ti catalyst exhibited higher activity than V1Ti catalyst in the absence or presence of H_2O. The doping of K led to the decreased activities of both catalysts. However, the NO_x conversion over V0.5Ce5Ti was much higher than that of V1Ti catalyst. The alkali-resistance of V0.5Ce5Ti is significantly higher than that of V0.5W5Ti catalyst. These enhanced performance stemmed from the existed redox cycle ($V^{4+} + Ce^{4+} \leftrightarrow V^{5+} + Ce^{3+}$). In situ DRIFTS measurements revealed that the existence of Ce on the V0.5Ce5Ti catalyst can promote the formation of NO_2 and monodentate nitrate species, both of which were reactive intermediates for the NH_3-SCR of NO_x.

Acknowledgments

This research was financially supported by the National Natural Science Foundation of China (21377010, 21325731) and the Program for New Century Excellent Talents of the Chinese Ministry of Education (NCET-13-0650).

Appendix A. Supplementary data

Supplementary material related to this article can be found, in the online version, at http://dx.doi.org/10.1016/j.apcatb.2014.03.049.

References

[1] Z. Liu, S.I. Woo, Catal. Rev.—Sci. Eng. 48 (2006) 43–89.
[2] G. Busca, L. Lietti, G. Ramis, F. Berti, Appl. Catal., B: Environ. 18 (1998) 1–36.
[3] Z. Huang, X. Gu, W. Wen, P. Hu, M. Makkee, H. Lin, F. Kapteijn, X. Tang, Angew. Chem. Int. Ed. 52 (2013) 660–664.
[4] S. Putluru, A. Jensen, A. Riisagera, R. Fehrmann, Catal. Sci. Technol. 1 (2011) 631–637.
[5] F. Tang, B. Xu, H. Shi, J. Qiu, Y. Fan, Appl. Catal., B: Environ. 94 (2010) 71–76.
[6] G. Qi, R.T. Yang, J. Catal. 217 (2003) 434–441.
[7] G. Qi, R.T. Yang, R. Chang, Appl. Catal., B: Environ. 51 (2004) 93–106.
[8] H. Liu, L. Wei, R. Yue, Y. Chen, Catal. Commun. 11 (2010) 829–833.
[9] L. Chen, J. Li, M. Ge, J. Phys. Chem. C 113 (2009) 21177–21184.
[10] Y. Peng, J. Li, W. Shi, J. Xu, J. Hao, Environ. Sci. Technol. 46 (2012) 12623–12629.
[11] W. Shan, F. Liu, H. He, X. Shi, C. Zhang, Chem. Commun. 47 (2011) 8046–8048.
[12] W. Shan, F. Liu, H. He, X. Shi, C. Zhang, Appl. Catal., B: Environ. 115 (2012) 100–106.
[13] H.L. Koh, H.K. Park, J. Ind. Eng. Chem. 19 (2013) 73–79.
[14] N.Y. Topsøe, Science 265 (1994) 1217–1219.
[15] S.B. Kristensen, A.J. Kunov-Kruse, A. Riisager, S.B. Rasmussen, R. Fehrmann, J. Catal. 284 (2011) 60–67.
[16] P. Li, Y. Xin, Q. Li, Z. Wang, Z. Zhang, L. Zheng, Environ. Sci. Technol. 46 (2012) 9600–9605.
[17] L. Chen, J. Li, M. Ge, L. Ma, H. Chang, Chin. J. Catal. 32 (2011) 836–841.
[18] P.G.W.A. Kompio, A. Brückner, F. Hipler, G. Auer, E. Löffler, W.A. Grünert, J. Catal. 286 (2012) 237–247.
[19] B. Thirupathi, P.G. Smirniotis, Appl. Catal., B: Environ. 110 (2011) 195–206.
[20] D. Yang, L. Wang, Y. Sun, K. Zhou, J. Phys. Chem. C 114 (2010) 8926–8932.
[21] V.I. Bukhtiyarov, Catal. Today 56 (2000) 403–414.
[22] J. Mendialdua, R. Casanova, Y. Barbaux, J. Electron. Spectrosc. 71 (1995) 249–261.
[23] M. Kang, E.D. Park, J.M. Kim, J.E. Yie, Appl. Catal., A: Gen. 327 (2007) 261–269.
[24] Z. Wu, R. Jin, Y. Liu, H. Wang, Catal. Commun. 9 (2008) 2217–2220.
[25] F. Liu, H. He, Y. Ding, C. Zhang, Appl. Catal., B: Environ. 93 (2009) 194–204.
[26] L. Lietti, I. Nova, G. Ramis, L. Dall'Acqua, G. Busca, E. Giamello, P. Forzatti, F. Bregani, J. Catal. 187 (1999) 419–435.
[27] M.A. Larrubia, G. Ramis, G. Busca, Appl. Catal., B: Environ. 27 (2000) L145–L151.

[28] L. Dall'Acqua, I. Nova, L. Lietti, G. Ramis, G. Busca, E. Giamello, Phys. Chem. Chem. Phys. 2 (2000) 4991–4998.
[29] D.A. Peña, B.S. Uphade, E.P. Reddy, P.G. Smirniotis, J. Phys. Chem. B 108 (2004) 9927–9936.
[30] L. Chen, J.H. Li, M.F. Ge, Environ. Sci. Technol. 44 (2010) 9590–9596.
[31] A. Trovarelli, Catal. Rev.—Sci. Eng. 38 (1996) 439–520.
[32] G.M. Underwood, T.M. Miller, V.H. Grassian, J. Phys. Chem. A 103 (1999) 6184–6190.
[33] Y. Chi, S.S.C. Chuang, Catal. Today 62 (2000) 303–318.
[34] Z. Liu, S.I. Woo, W.S. Lee, J. Phys. Chem. B 110 (2006) 26019–26023.
[35] N.Y. Topsøe, J.A. Dumesic, H. Topsøe, J. Catal. 151 (1995) 241–252.
[36] H. Bosch, F. Janssen, Catal. Today 2 (1988) 369–379.
[37] A.V. Salker, W. Weisweiler, Appl. Catal., A: Gen. 203 (2000) 221–229.
[38] G. Centi, S. Perathoner, J. Catal. 152 (1995) 93–102.
[39] T.S. Park, S.K. Jeong, S.H. Hong, S.C. Hong, Ind. Eng. Chem. Res. 40 (2001) 4491–4495.
[40] W.S. Kijlstra, D.S. Brands, H.I. Smit, E.K. Poels, A. Bliek, J. Catal. 171 (1997) 219–230.
[41] M. Koebel, M. Elsener, G. Madia, Ind. Eng. Chem. Res. 40 (2001) 52–59.
[42] G. Ramis, G. Busca, F. Bregani, P. Forzatti, Appl. Catal. 64 (1990) 259–278.